

Cite this: DOI: 10.1039/c1cs15057j

www.rsc.org/csr

## TUTORIAL REVIEW

## DNA origami: a quantum leap for self-assembly of complex structures†

Thomas Tørring,<sup>a</sup> Niels V. Voigt,<sup>a</sup> Jeanette Nangreave,<sup>b</sup> Hao Yan<sup>\*b</sup> and Kurt V. Gothelf<sup>\*a</sup>

Received 2nd March 2011

DOI: 10.1039/c1cs15057j

The spatially controlled positioning of functional materials by self-assembly is one of the fundamental visions of nanotechnology. Major steps towards this goal have been achieved using DNA as a programmable building block. This *tutorial review* will focus on one of the most promising methods: DNA origami. The basic design principles, organization of a variety of functional materials and recent implementation of DNA robotics are discussed together with future challenges and opportunities.

## Introduction

In the field of nanotechnology, one of the most immediate challenges is to develop strategies to precisely control and organize various functional materials. During the past 30 years DNA nanotechnology has gradually evolved to provide solutions to this challenge. In particular, the work of Seeman *et al.* has established DNA structures as versatile building blocks for complex nanoscale assembly; from the first reports on immobile Holliday junctions,<sup>1</sup> a cubic cage,<sup>2</sup> and two dimensional lattices,<sup>3</sup> to the vision of a three dimensional DNA crystal which was realised in 2009.<sup>4</sup>

The complexity and size of self-assembled DNA nanostructure building blocks were radically increased after a report published by Rothemund in 2006.<sup>5</sup> He introduced the basic principles of the so-called DNA origami method. Origami refers to the Japanese art of transforming a flat sheet of paper into an arbitrarily shaped object through folding and sculpting techniques. In DNA origami a long single strand of DNA (scaffold) is folded into arbitrary shapes by hundreds of short synthetic oligonucleotides, referred to as staple strands. Each of the staple strands is designed to bind to different places along the scaffold, thereby bringing these otherwise distant points into close proximity. Collectively, the staple strands determine the precise size and shape of the final, compact structure. Rothemund illustrated the versatility of the concept by designing a number of different structures.

The main reason for the immediate success of DNA origami is the experimental simplicity and fidelity of the folding process. With few exceptions,<sup>6</sup> almost all earlier assemblies were composed of multiple short DNA oligonucleotides (oligos) only, which required very precise stoichiometry and purification of individual oligos to obtain reasonable yields.

<sup>a</sup> Danish National Research Foundation: Centre for DNA Nanotechnology, at the Interdisciplinary Nanoscience Center and the Department of Chemistry, Aarhus University, Langelandsgade 140, 8000 Aarhus C, Denmark. E-mail: kvg@chem.au.dk; Fax: +45 86196199; Tel: +45 89423907

<sup>b</sup> Department of Chemistry and Biochemistry & The Biodesign Institute, Arizona State University, Tempe, AZ, USA. E-mail: hao.yan@asu.edu; Fax: +1 480 727 2378; Tel: +1 480 727 8570

† Part of a themed issue on the advances in DNA-based nanotechnology.



Thomas Tørring

Thomas Tørring was born in Aalborg, Denmark, in 1983. He received his BSc in nanoscience from Aarhus University in 2006 and is currently finishing his PhD studies in the group of Kurt Gothelf. His research interests include DNA Origami and DNA-protein conjugation.



Niels V. Voigt

Niels V. Voigt was born in Skanderborg, Denmark, in 1983. He received his BSc in nanoscience from Aarhus University in 2006 and is currently finishing his PhD studies in the group of Kurt V. Gothelf. Part of his research was conducted in the laboratories of Prof. William Shih at Harvard Medical School. His interests include DNA Origami, computational modeling and renewable energy.

The use of a long scaffold strand in DNA origami alleviates the stoichiometry concerns, as the short staple strands can be applied in excess and can be used as synthesised without additional purification. These advances have made it possible to form uniform structures of significantly higher complexity and, at least for two dimensional (2D) origami structures, with impressive high yield within hours.

Each of the staple strands has a unique sequence and its position in the assembled structure is determined by the design. Staple strands are made by automated DNA synthesis and are commercially available. They can be obtained with chemical modifications and this allows the facile introduction of a variety of different functionalities that are displayed at predetermined positions in the final structure.

## Design

The basic structural motif of DNA origami, the antiparallel crossover, has been widely used in the field of DNA nanotechnology, since it was first reported by Fu and Seeman.<sup>7</sup> It was demonstrated that this motif could align DNA helices in a parallel orientation when multiple crossovers on the same side

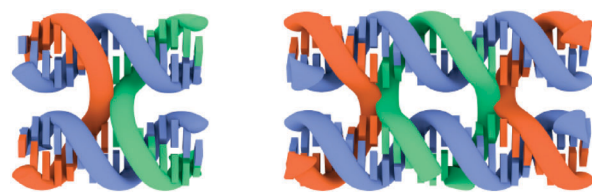


**Fig. 1** Left: an immobile Holliday-junction, representing a single cross-over between two double helices. Right: the most common motif in DNA nanotechnology; an antiparallel double crossover.

of each helix were used to connect them. These constructs were generally termed “tiles” (a minimal example is shown in the right of Fig. 1) and were often designed to self-assemble into very large arrays.

In the original DNA origami designs, the 7249 nt single stranded scaffold originated from the bacteriophage M13mp18. In one example a rectangular DNA origami with dimensions of 90 nm × 60 nm was assembled with 225 staple strands, most of which were 32 nts long. The 32 helices in the folded origami structure were connected by more than 200 crossovers. An excess of 5 to 10 equivalents of each staple compared to the scaffold was used, resulting in correct assembly of the rectangular structure with nearly 90% yield in less than 2 hours.

In a naturally occurring B-DNA helix, there are approximately 10.5 base pairs per turn (bps/turn). Rothemund's first origami designs positioned the crossovers 16 bps, or close to 1.5 helical turns, apart to achieve a 180° change in direction. The resulting helices were aligned in parallel in an almost coplanar structure. As the number of base pairs defines the angle between two crossovers, changing this number will move the effected helix out of the plane. This principle is demonstrated in a six helix bundle<sup>8</sup> and generalised (Fig. 2) to create a variety of 3D shapes by Shih and co-workers.<sup>9</sup>

The earliest DNA origami designs were prepared by hand and/or by various in-house, purpose-specific software. This was a tedious, error prone and time-consuming process until more generic software packages were developed. The first origami design program published was a plug-in to the sequence



**Jeanette Nangreave**

*Jeanette Nangreave was born in Rochester, NY, USA in 1979. She received her BS in chemistry from the University of South Carolina in 2006 and is currently finishing her PhD studies in the Yan research group at Arizona State University. Her research interests include using DNA nanostructures to model the binding behavior of polyvalent molecules to determine the structural parameters that affect binding stability and dynamics.*



**Hao Yan**

*Hao Yan was born in 1971 in China and studied chemistry at Shandong University, China. He performed his PhD in structural DNA nanotechnology under Professor N. C. Seeman, New York University. Following a period as an Assistant Research Professor at Duke University, he joined Arizona State University as Assistant Professor in 2004. He became a Full Professor at Arizona State University since 2008. The themes of his research are structural DNA nanotechnology and DNA-directed self-assembly.*



**Kurt V. Gothelf**

*Kurt Vesterager Gothelf was born in 1968 in Denmark and studied chemistry at Aarhus University, Denmark and at Heidelberg University, Germany. He performed his PhD in organic synthesis and asymmetric catalysis under Professor K. A. Jørgensen, Aarhus University. Following a period as a post doc. at Aarhus University he joined Professor M. C. Pirrung's group at Duke University, USA. From May 2002 he has been an Associate Professor at Aarhus University and in August 2007 he was appointed Professor in organic nanochemistry. In 2007 Kurt Gothelf became Director of the Danish National Research Foundation Centre for DNA Nanotechnology.*



**Fig. 2** Distances between crossovers define the angle between helices. Left: an integer number of half turns results in a 2D structure. Right: a non-integer number of half turns results in a 3 dimensional structure. In this case an angle of  $120^\circ$  is achieved by a 7 base pair distance between crossovers.

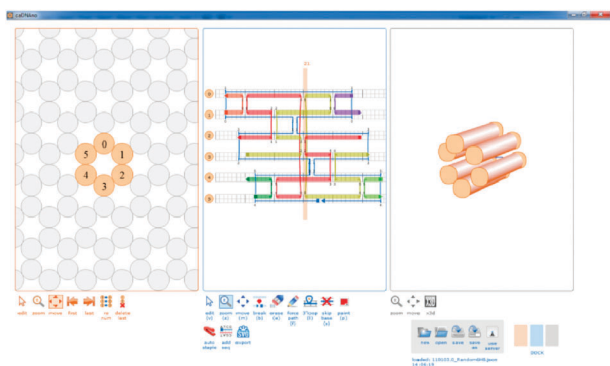


**Fig. 3** A screenshot from the caDNAno software.<sup>11</sup> The program provides a facile and intuitive interface for designing DNA origami structures.

editing program SARSE.<sup>10</sup> The SARSE application lets the user import bitmap images and fills them with DNA to create 2D origami shapes. This was demonstrated by the design and assembly of a dolphin structure. Later on, a more accessible program, caDNAno,<sup>11</sup> was released. At first, it was primarily intended for the design of 3D-DNA origami with the helices organised in honeycomb arrangements (Fig. 3). In this program, the user schematically weaves the scaffold through the structure, and the program subsequently suggests a routing pattern for the staple strands. The staples can be adjusted before the scaffold sequence is assigned and the staple sequences are generated. More recently, a caDNAno version with the DNA helices organised in square patterns was published.<sup>12</sup> This also enables the design of the original 2D structures in addition to the new, 3D structures.

### The structure race

In the original report of the 2D-DNA origami,<sup>5</sup> the generality of this DNA folding technique was demonstrated by the construction of a multitude of different 2D geometries (Fig. 4) with high folding yields. The addressability of DNA origami was illustrated through the display of DNA dumbbell loops protruding at predetermined locations on one surface of the structures. These dumbbell loops allowed the author to distinguish otherwise topologically equivalent parts of the structures.

Several additional groups constructed other 2D origami shapes<sup>10,13</sup> and after a productive period with many reports of related 2D structures, a series of papers describing more advanced 3D structures were published in 2009.

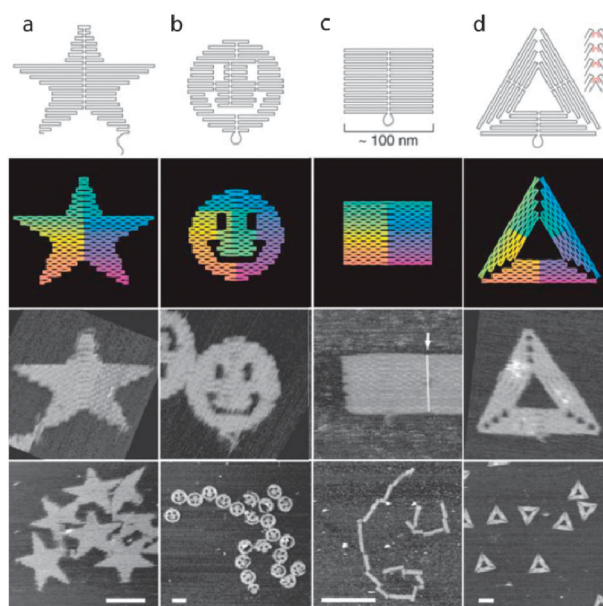


**Fig. 4** The first examples of the versatile DNA Origami technique. The upper panel illustrates the designs. The lower panels contain the resulting DNA structures as imaged by AFM. Scale bars are 100 nm for a, b, d and 1  $\mu\text{m}$  for c. Adapted by permission from MacMillan Publishers Ltd: ref. 5, copyright 2006.

One way of extending from 2D to 3D is to connect several planar origami sub-structures at the edges. Each plane can be held at an angle to adjacent planes to afford a 3D superstructure. This principle was demonstrated by Kjems, Gothelf and coworkers<sup>14</sup> in a report on the formation and thorough characterisation of a DNA origami box with a controllable lid. Two faces of the box were hinged along one edge and held closed along the opposite edge by pairs of hybridised staples (locks). One staple from each lock contained a toehold which could release the lid by adding the complimentary oligo (key) to the solution. The structure of the DNA box was confirmed by small angle X-ray scattering (SAXS), dynamic light scattering (DLS), AFM and cryo-TEM. Moreover, the opening and closing of the lid were confirmed by FRET experiments as illustrated in Fig. 5.

Kuzuya and Komiyama<sup>15</sup> and Sugiyama *et al.*<sup>16</sup> have also reported box structures with similar design features and Yan<sup>17</sup> and co-workers used a related strategy to construct a hollow DNA origami tetrahedron. The 2009 paper by Shih and co-workers reported a new set of design principles for 3D origami construction. Rather than hollow structures, the origami were more dense with a design based on the parallel arrangement of helices into a honeycomb lattice<sup>9</sup> (Fig. 6a). The design principles in the latter publication are more generally applicable, however, the tradeoffs are significantly longer assembly times and considerably lower yields for the more complex structures. Recently Shih and co-workers have reported on strong improvements on purification yields of these complex assemblies.<sup>18</sup> Yan, Shih and co-workers described a more compact design for 3D origami with the layers of helices packed on a square lattice.<sup>12</sup> A square lattice provides a natural framework for rectangular objects and several cuboid structures were demonstrated (Fig. 6b).



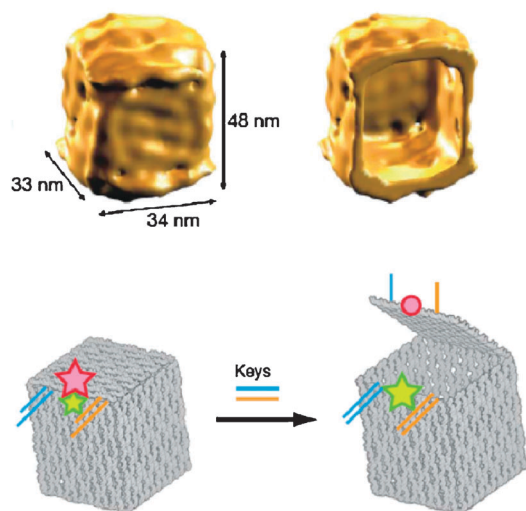


**Fig. 5** Top: single molecule reconstruction of the DNA box from cryo-TEM. The image clearly shows the cavity within the box. Bottom: the controlled opening of the lid upon addition of DNA keys was demonstrated by FRET. Adapted by permission from MacMillan Publishers Ltd: ref. 14, copyright 2009.

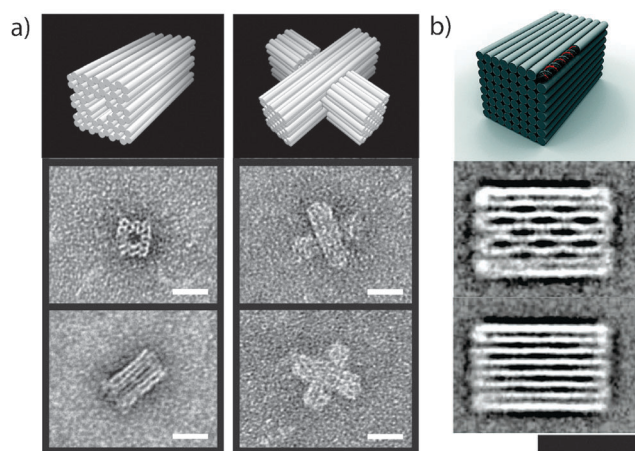


**Fig. 6** Three dimensional DNA origami structures. (a) Two examples of the 3D structures created by Shih and co-workers in 2009.<sup>9</sup> The structures were designed using the honey comb lattice previously described. Adapted by permission from MacMillan Publishers Ltd: ref. 9, copyright 2009. (b) Yan and co-workers<sup>12</sup> reported a more compact design for 3D origami using layers of helices packed on a square lattice. Adapted with permission from ref. 12. Copyright 2009 American Chemical Society.

Following the construction of compact DNA structures based on a honeycomb pattern, Shih and co-workers published a report of the design of twisted and bent origami structures.<sup>19</sup> As previously mentioned, B-DNA contains 10.5 bps per helical turn. Designing 3D structural units with more or less than 10.5 bps per turn in certain helices results in a global twist (see Fig. 7a). Locally, the effect of fewer than 10.5 bps/turn is an over-wound helix that exerts a left hand torque on the structure surrounding it. If many over-wound helices are present in a structure, the forces add up to create a global twist. To study and quantify this twisting, the researchers designed 3D blocks of DNA origami containing helices with more or less than 10.5 bps/turn, and examined their

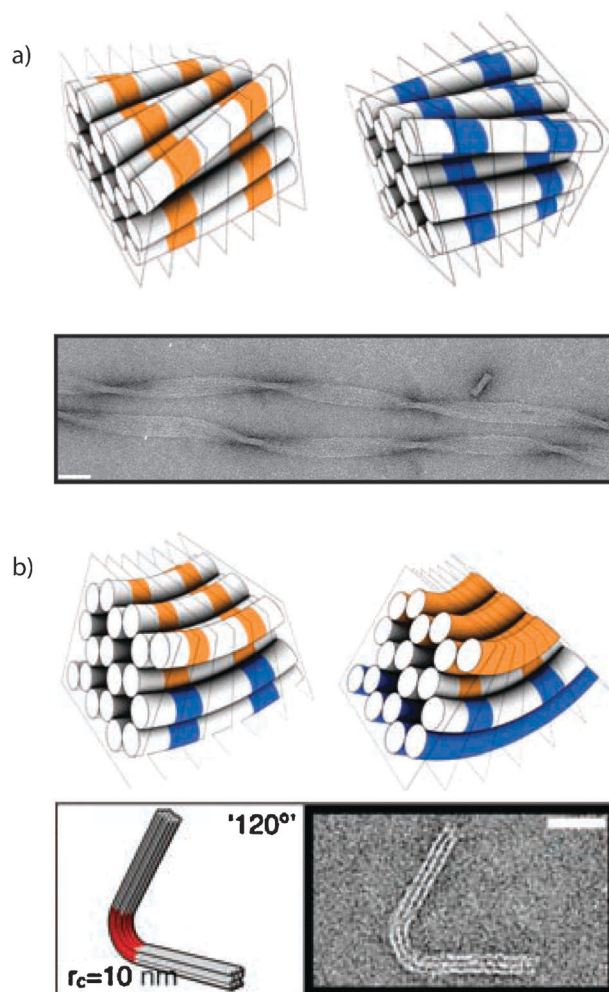


**Fig. 7** Twist and curvature can be introduced in the origami structures by adjusting the number of base pairs between crossovers. (a) In structures designed with fewer than 10.5 bps/turn, an overall left-handed twist is observed. In structures with more than 10.5 bps/turn, an overall right-handed twist is observed. (b) When combined, the twist strain is balanced and an overall curvature is observed. Scale bars are 20 nm. From ref. 19. Adapted with permission from AAAS.

polymerisation into longer ribbons. These ribbons were subsequently stained and imaged by TEM to measure the characteristic dimensions and deduce the twist of the building blocks. Additionally, they demonstrated that it is feasible to have both under- and over-wound segments in the same DNA origami structure. If the segments were part of the same cross-section of the structure, the twist could be balanced. By carefully designing each element of the structure, an overall bend could be imposed. Precise control over the degree of bending was demonstrated in a series of structures which are shown in Fig. 7b. Furthermore, they assembled a number of higher order assemblies comprised of bent origami. Applying the knowledge gained in these studies to the earlier 2D structures, it is apparent that they probably exhibit an overall twist in solution, as their design is based on 10.67 bps/turn. This could explain the convex and concave sides of the DNA box when observed by cryo-TEM, as seen in Fig. 5.

Recently, Yan and co-workers reported a strategy to design and construct 3D DNA origami structures that contain highly

curved surfaces.<sup>20</sup> In a departure from a rigid lattice model, their method involves defining the surface features of a target object with the scaffold, followed by manipulation of DNA conformation and identification of ideal positions for strand crossovers. Concentric rings of DNA are used to generate in-plane curvature, constrained to 2D by rationally designed geometries and crossover networks. Out-of-plane curvature is introduced by adjusting the particular position and pattern of crossovers between adjacent DNA double helices, whose conformation often deviates from the natural, B-form twist density. A series of DNA nanostructures with high curvature—such as 2D arrangements of concentric rings and 3D spherical shells, ellipsoidal shells, and a nanoflask—were assembled. With the nanoflask, they demonstrated that in and out of plane curvature can be simultaneously adjusted to achieve asymmetric objects with elaborate structural elements, including varying curvature and diameter (Fig. 8). Their method should allow the construction of objects with complex features, as is characteristic of most biological molecules. In addition, their report improves our ability to control the intricate structure of DNA nano-architectures and create more diverse building blocks for molecular engineering.

Another tool in the assembly of larger 3D origami structures is the use of single stranded regions of the scaffold as entropic springs. This was developed by Shih and co-workers with the construction of so-called tensegrity structures (see Fig. 9).<sup>21</sup> Tensegrity is a well-known engineering principle used to construct lightweight structures from compressed (rigid) beams connected by stress-bearing wires. When applied to DNA origami, the scaffold is used to generate the rigid beams, together with the staple strands, but also as the stress-bearing wires. This enables control of the relative orientation of the beams without any additional connection between them. In the study, the length of the wires was varied to demonstrate that the structure would collapse without sufficient stress on the wires. On the other hand, overly shortened single stranded

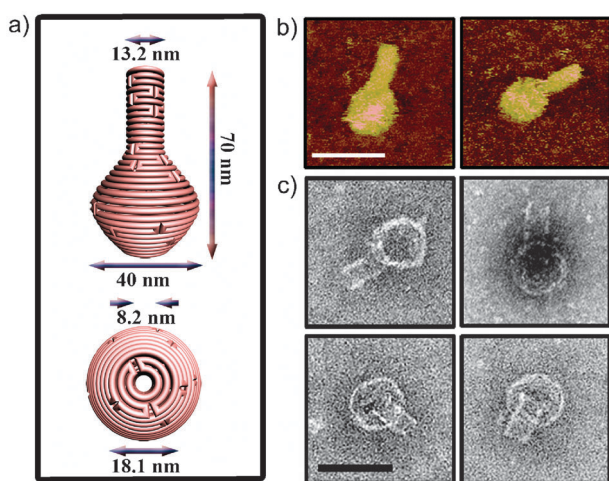


**Fig. 8** Double helical DNA is bent to follow the rounded contours of the target object, held in place by rationally designed crossover networks. (a) Schematic representation of the nanoflask with dimensions indicated. (b) AFM images of the nanoflask. Scale bar is 75 nm. (c) TEM images of the nanoflask after random deposition on TEM grids. Scale bar is 50 nm. From ref. 20. Adapted with permission from AAAS.

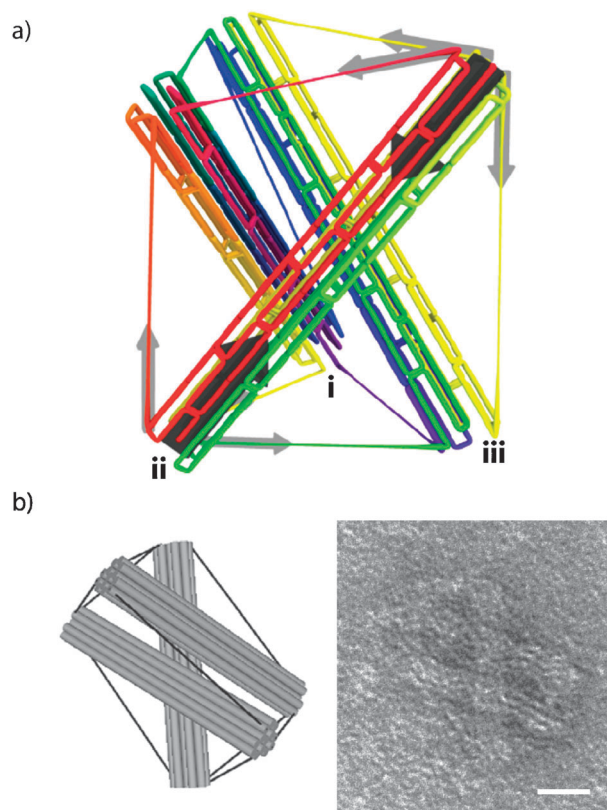


**Fig. 9** Single stranded regions of the scaffold can be used as entropic springs to define the spatial arrangement of rigid origami beams. (a) Routing of the scaffold through the structure. (b) Model and TEM image of the final structure. The scale bar is 20 nm. Adapted by permission from MacMillan Publishers Ltd: ref. 21, copyright 2010.

connections also resulted in misfolded structures. The rigidity of the beams was investigated by adjusting the number of helices in the bundles.

As arbitrarily shaped 3D structures were becoming increasingly accessible, the focus shifted from structural elements to reconfigurability. Yan and co-workers reported the design and assembly of quasi-2D DNA origami structures with overall Möbius topology (Fig. 10).<sup>22</sup> This topology necessitated only six individual parallel helices and as such only six scaffold crossovers were required. Even though the design implies a significant degree of twist and curvature, the DNA throughout the structure adopted 10.67 bps/turn. This is further demonstration of the flexibility and vigour of the origami method. An inherent property of the structure is chirality, and while the researchers were expecting to observe a strong preference for the right handed structure, owing to the  $>10.5$  bps/turn,<sup>19</sup> they only observed a 1.4 : 1 excess of the expected isomer. After confirming the assembly, the researchers altered the design to include a seam, which could be opened by strand displacement. Depending on the position of the seam, different structures could be made from an original Möbius band, one of which was a catenane with two interlocked rings.

Another objective for the development of DNA nanostructures is to expand the size of the assemblies. So far the size has been limited by the length of the scaffold, where 7 kilobase assemblies have become the standard due to the accessibility of the single



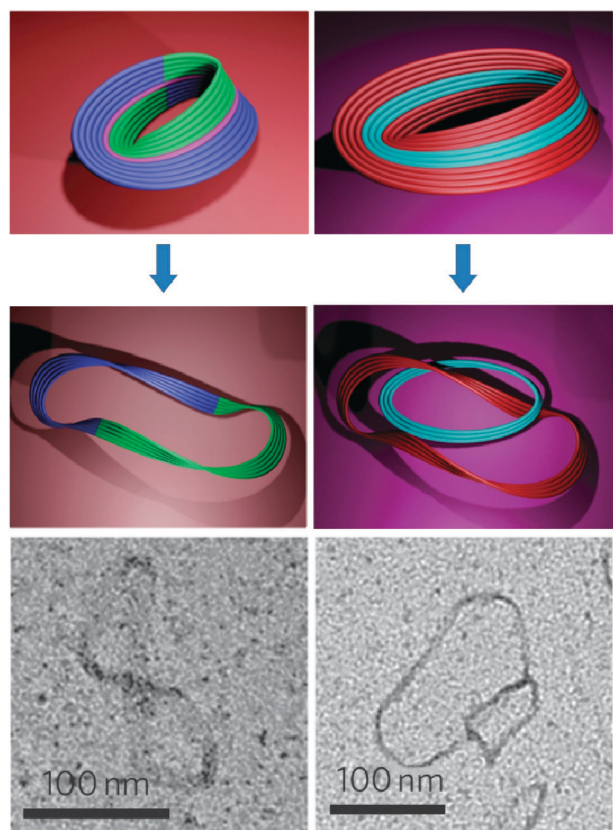


**Fig. 10** Topologically reconfigurable structures. Top: two Möbius bands. Bottom: after addition of displacement strands, the Möbius bands are reconfigured into a ring with two full twists and twice the circumference as the original (left), or into two interlocked rings where one remains a Möbius strip (right). Adapted by permission from MacMillan Publishers Ltd: ref. 22, copyright 2010.

stranded genome from the bacteriophage M13mp18. One method to circumvent this was reported by Woolley and co-workers.<sup>23</sup> They used biotinylated primers in a PCR reaction and subsequently isolated the long single stranded PCR products. The products were employed as scaffolds in the assembly of large origami structures. If much longer scaffolds are to be used the number of staple strands would also drastically increase. Labean and co-workers have demonstrated the use of high quality mixed oligo pools for this purpose.<sup>24</sup>

Various other approaches to create larger structures have also been investigated within the past few years. These have included: algorithmic assembly from a origami seed,<sup>25,26</sup> origami oligomerisation<sup>27</sup> and polymerisation,<sup>28</sup> 8-helix bundle staples<sup>29</sup> and the use of double stranded genomes as scaffolds.<sup>30</sup> For algorithmic self-assembly, the high level of information contained in an origami structure was exploited to create an origami seed, from which a traditional algorithmic tile was grown. Although it is not the main purpose of the approach, the size of the final structure is significantly increased, but at the cost of spatial addressability and resolution.

The most significant challenge of using larger genomes as scaffolds is that the vast majority of these are double stranded DNA. Shih and co-workers reported the successful one-pot assembly of two different origami structures from a single double stranded scaffold (7560 bps). To achieve this assembly,

the DNA mixture was first completely denatured by a combination of heat and formamide (40%), a method developed together with the Simmel group,<sup>31</sup> to achieve complete separation of the forward and reverse scaffold strands. When denatured, the mixture was quickly cooled to room temperature to allow the faster hybridisation of the staple strands and kinetically trap the scaffolds. The remaining annealing of the structures was achieved by gradually removing the formamide by dialysis. Although this technique holds promise for the use of larger double stranded scaffolds, no such results have yet been published.

Another route to assemble larger structures is the use of more complex staples. Liu and co-workers<sup>29</sup> reported the use of 8-helix tiles as staples rather than traditional, single stranded oligos. This enabled the construction of assemblies of more than 30 000 bps, which were theoretically fully addressable. It is foreseeable that larger DNA tiles such as DNA origami itself can also serve as staples in such strategy to scale up DNA origami assembly, while this would require stepwise assembly processes which may affect the overall yield.

An attempt to form well-defined 2D lattices was reported by Liu and co-workers.<sup>32</sup> In the study they extrapolated traditional DNA tile design assembly strategies to build larger origami

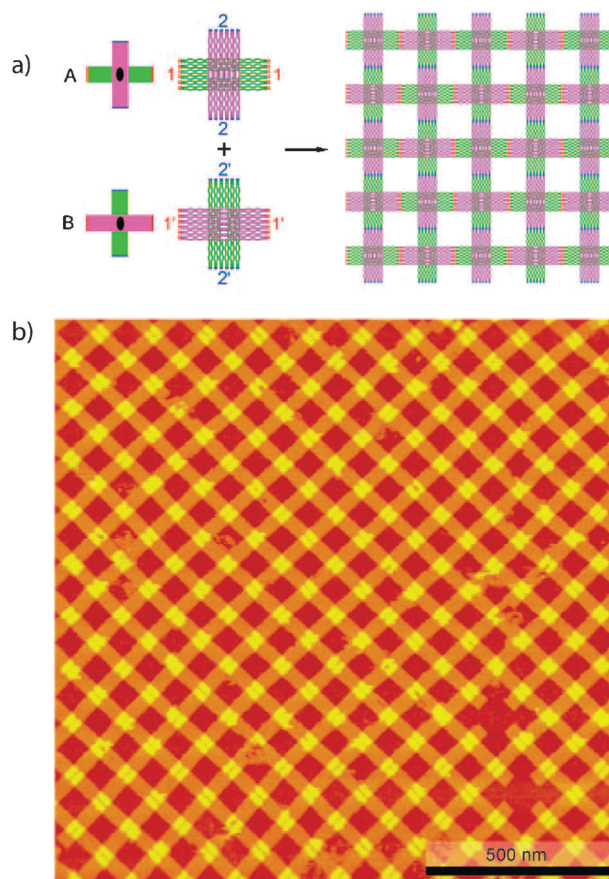


**Fig. 11** Two dimensional crystals from DNA origami tiles. (a) Two unique origami structures A and B with complementary ends are designed to form 2D arrays. (b) The assembled arrays as imaged by AFM. Adapted from *Crystalline two-dimensional DNA-origami arrays*, ref. 28. Copyright Wiley VCH Verlag GmbH & Co KGaA. Reproduced with permission.

arrays. The significantly larger size and higher flexibility of the unit building blocks allowed the 2D origami arrays to bend and fold back on themselves. Various tubes and one-dimensional two-layer polymeric assemblies were the main product.

The successful polymerisation of two dimensional origami structures was achieved by Seeman and co-workers.<sup>28</sup> They found that the key design feature is orientation of the helices. It is well-known that the ends of helices have a tendency to stack and cause nonspecific polymerisation of origami in one direction. In most origami structures this outcome is prevented by adding single stranded loops at the ends of selected helices. Seeman and co-workers exploited the stacking effect by using a symmetric cross-like design with helical axes propagating in two perpendicular directions as shown in Fig. 11a. This led to a large regular lattice of DNA origami (Fig. 11b).

### From structure to functionalisation

Beyond the many structural advances that have been reported, there has been great progress in generating functional DNA origami systems. As previously described, an attractive feature of DNA origami is the unique position of every staple strand within the assembled structure. The potential for DNA origami to function as a molecular pegboard immediately gained great interest.

One of the first reported DNA origami applications was the development of a label-free RNA sensor by Yan and co-workers<sup>33</sup> (Fig. 12a). They simply extended the end of specific staples with sequences designed to bind RNA segments of biological interest. The hybridisation between the staple extensions and the RNA targets created local protrusions from the origami surface that were readily imaged by AFM. They also incorporated a barcode system that enabled the one-pot, simultaneous detection of multiple targets. More recently, a similar nucleic acid sensor was demonstrated by Fan and co-workers.<sup>34</sup> Seeman and co-workers recently reported the use of DNA origami for single nucleotide polymorphism (SNP) detection that the SNP signal can be visually displayed at the single molecule level<sup>35</sup> (Fig. 12b). Indeed, the DNA origami could serve for potential applications in single cell proteomics as it has the advantage of being water soluble and spatially addressable at nanoscale compared to solid surface based microarray chips.

The Yan group also used DNA origami to study distance dependent aptamer–protein binding.<sup>36,37</sup> Aptamer modified staples were displayed on the surface of rectangular DNA origami, with precise control over the distance between two lines of aptamers (Fig 13). This enabled the researchers to determine the optimal distance for bi-valent binding.

A multitude of other materials have been conjugated to DNA origami structures. These include silver nanoparticles,<sup>38</sup> gold nanoparticles,<sup>39–42</sup> carbon nanotubes,<sup>43</sup> quantum dots,<sup>41</sup> dendrimers,<sup>44</sup> virus capsids,<sup>45</sup> streptavidin<sup>46–48</sup> and Ni-NTA bound to His-tagged proteins.<sup>49</sup> The common feature of each of these reports is that they exploit the unique addressability of DNA origami. Staple strands are easily modified either chemically during synthesis or by batchwise enzymatic labelling<sup>50</sup> to specifically bind various targets. These and the origami scaffolds are subsequently assembled and analysed.

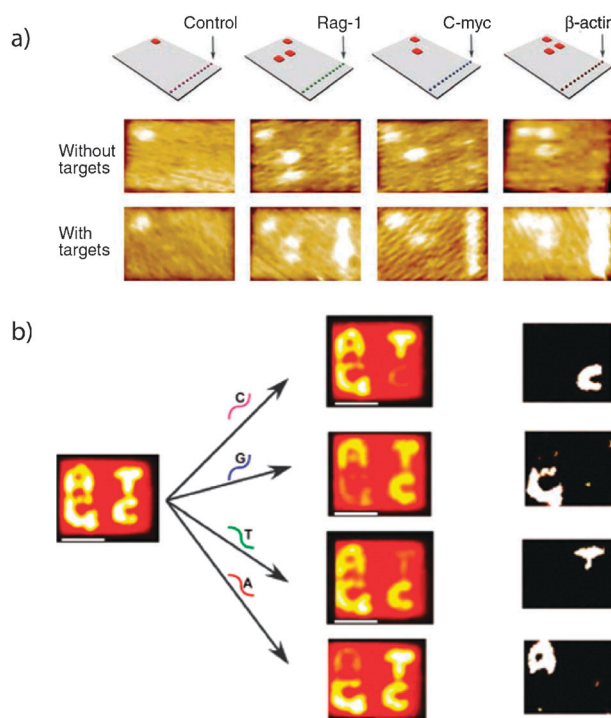


**Fig. 12** (a) An RNA sensor based on hybridization of the targets to single stranded extensions of staple strands. Unique barcodes enable the simultaneous, multiplex analysis of several targets. From ref. 33. Adapted with permission from AAAS. (b) A DNA origami based molecular chip to detect SNP with visual output imaged by AFM. Adapted with permission from ref. 35. Copyright 2011 American Chemical Society.

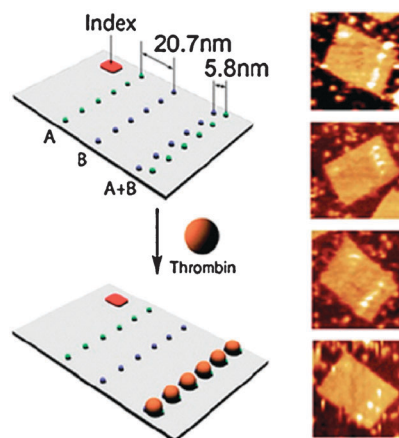


**Fig. 13** Exploiting the predictable structure of DNA origami to control the distance between two different aptamers to bind a protein target. Adapted by permission from MacMillan Publishers Ltd: ref. 37, copyright 2010.

For many of the proposed applications of DNA origami and potential integration in functional systems such as CMOS based circuitry, it is of tremendous importance to be able to precisely control the deposition (position and orientation) of the origami. One way to accomplish this is to trap the origami structures between electrodes using dielectrophoresis.<sup>51</sup> More recently, a parallel lithographic method was developed and refined.<sup>52,54</sup> The method involves selective etching of a hydrophilic pattern on an otherwise hydrophobic surface.



The negatively charged origami structures were found to selectively bind to these patterns, thereby providing control over position, orientation and thus the overall pattern of chemical modifications of the origami structure. An example of the latter is shown in Fig. 14. An alternative route that has been explored is the selective deposition and adsorption of DNA origami to silicon bound gold islands.<sup>53,55</sup> Yan and co-workers used fixed length DNA origami nanotubes, modified with multiple thiol groups near both ends, to connect surface patterned gold islands.<sup>53</sup> The nanotubes were efficiently aligned between the islands with various interisland distances and relative orientations. In addition, several interesting investigations have been reported on the metallization of origami structures. Strategically placed carbohydrates have been used as seeds for a metallization mediated by Tollens reagent by Yan and co-workers.<sup>56</sup> A global metallization could be achieved by using a chemical crosslinking reagent, glutaraldehyde, and Tollens reagent as reported by Woolley and co-workers<sup>57</sup> or by seeding with cationic AuNP and enhancing with EM HQ Gold Enhance™ as described by Liedl and co-workers.<sup>58</sup> Each of these developments represents progress toward bridging bottom-up and top-down assembly approaches.

The ability to visualize single molecule chemical reactions using DNA origami as a platform was demonstrated by Gothelf and co-workers.<sup>59</sup> In their report, various functional groups were displayed on DNA origami that was adsorbed on a mica surface. Multiple washing steps and incubation with reagent mixtures facilitated the selective post-assembly chemical modification of the functionalised origami, including click-reactions and peptide bond formation. Biotin moieties were attached to the termini of the reaction products and the subsequent addition of streptavidin enabled visualisation by AFM (see Fig. 15). Furthermore, several different cleavable linkers were used to create various modification patterns. In the future, the incorporation of other proteins could expand

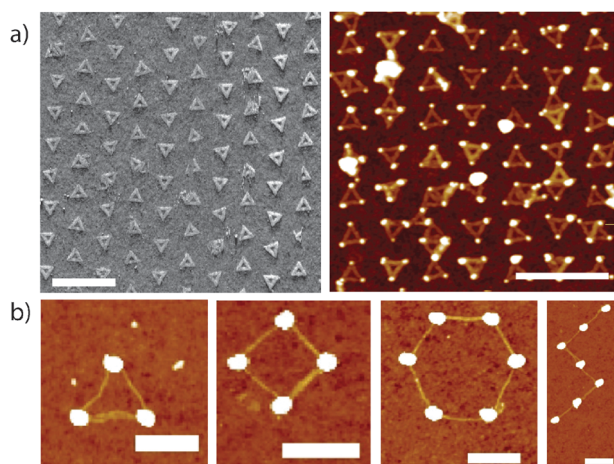


**Fig. 14** Precise control over the deposition of DNA origami. (a) Directing the position and orientation of origami triangles deposited on a surface by lithographic patterning. In the right image, the triangles have been modified with gold nanoparticles. Adapted by permission from MacMillan Publishers Ltd: ref. 52, copyright 2010. (b) Surface patterned gold islands are connected by DNA origami nanotubes. Adapted with permission from ref. 53. Copyright 2010 American Chemical Society.

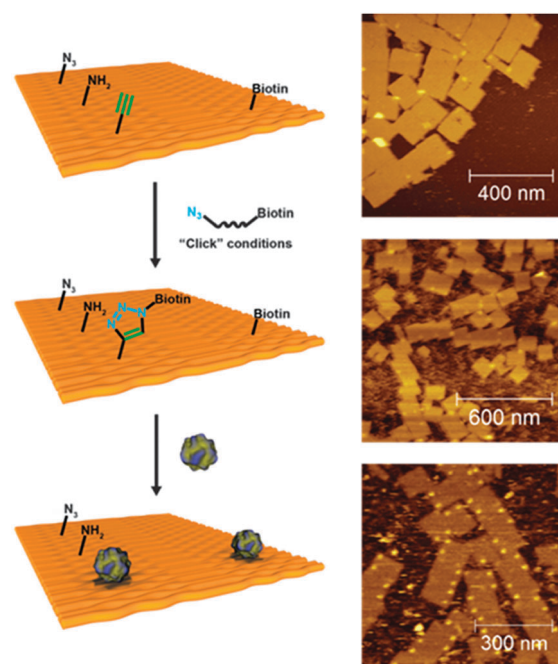


**Fig. 15** Several chemical functionalities are displayed on the surface of rectangular DNA origami and subsequent reaction efficiencies are read out *via* AFM with the addition of streptavidin. Adapted by permission from MacMillan Publishers Ltd: ref. 59, copyright 2010.

the scope of the technique. In addition to studying chemical bond and cleavage reactions, the same group<sup>60</sup> investigated the lifetime and migration distance of biologically relevant singlet oxygen through the chemical modification of staple strands organised with precise inter-molecular distances.

Niemeyer and co-workers<sup>61</sup> demonstrated that DNA origami can be functionalised with other classes of proteins, including the fusion proteins HaloTag® and Snap-Tag. The fusion proteins were shown to selectively bind to staples modified with the matching ligands. In a different report, alkaline phosphatase and horseradish peroxidase fusion proteins were used.<sup>62</sup> A DNA binding protein was investigated by Knudsen and co-workers.<sup>63</sup> Human topoisomerase I was captured by probes displayed on a DNA origami platform and AFM analysis was employed to identify the existence of secondary DNA binding sites.

The ability of DNA origami to position molecules at specific distances from one another was exploited for the development of a nanoscopic ruler for super resolution microscopy. Tinnefeld and co-workers<sup>64</sup> designed a rectangular origami with fluorophores incorporated at two corners. The fluorescent signal from the origami immobilised on a glass slide is restricted because the inter-fluorophore distance is smaller than the diffraction limit. They circumvented this limitation by using total internal reflection fluorescence (TIRF), a common super-resolution technique. The setup was used to determine the distance between the fluorophores displayed at the corners of the origami. The measured inter-fluorophore distance was  $88.2 \pm 9.5$  nm, compared to a predicted distance of 89.5 nm.

More recently, Simmel and co-workers<sup>65</sup> used a similar single molecule fluorescence technique called DNA-PAINT (DNA—point accumulation for imaging in nanoscale topography)



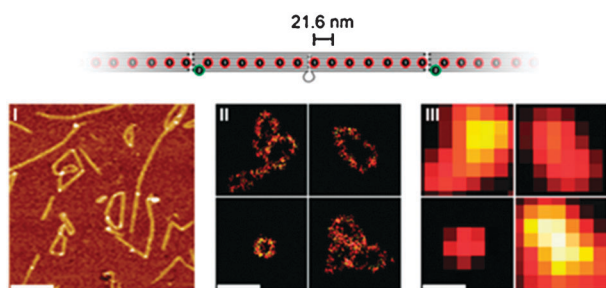


**Fig. 16** A long polymerising origami with binding sites for short fluorophore labelled oligonucleotide probes. This technique, termed DNA-PAINT, enables super resolution imaging without the disadvantage of bleaching. (I) An AFM-image of the assembled origami. (II) The super resolution reconstruction of the fluorophore binding events. (III) The diffraction limited raw data from the total internal reflection fluorescence microscope. Adapted with permission from ref. 65. Copyright 2011 American Chemical Society.

to analyse DNA origami. For the technique, various staple strands are extended with probes that are complementary to fluorescently labelled target oligos. The rate of association and dissociation of the oligos is studied and tuned by modulating the melting point of the complexes. Thus, the usual challenge of fluorophore bleaching associated with single molecule fluorescence experiments can be circumvented. Additionally, they demonstrated how the technique can be used to detect the presence of single staple strands in the origami. Fig. 16 shows the raw data and topographic reconstruction. Another interesting report from the group of Tinnefeld<sup>66</sup> was a complex four color FRET setup that was designed to monitor and control the energy transfer paths on a DNA origami. The energy from a donor dye could be transferred to one of two acceptors depending on the addition of a so-called “jumper” dye. Also rigid blocks of DNA origami have been used by Liedl and co-workers<sup>67</sup> to investigate and validate the distance dependence of the Förster theory.

## Dynamic systems

Beyond static structures, DNA origami presents the opportunity to construct and study dynamic arrangements of molecules. This has led to significant advances in molecular robotics and the study of enzymatic processes.

The development of high-speed AFM has allowed the study of enzymatic reactions<sup>68,69</sup> and molecular dynamics.<sup>70</sup> One example from Sugiyama and co-workers is shown in Fig. 17. They reported the formation and dissociation of a G-quadruplex upon the addition and removal of buffer containing KCl. A DNA origami frame structure was designed with two parallel helices bridging the inner cavity. Each helix contained a single stranded extension that, in the presence of potassium, formed a G-quadruplex. The transition from single strands to G-quadruplex was observed in real time. Similar frame structures were used to study a methyltransferase enzyme (*M.EcoRI*) and two DNA repair enzymes (hOgg1 and PDG). Two helices of different lengths were attached to opposite sides of the frame and the well-defined structure of the frame imposed a unique amount of tension on each helix. Each of the enzymes in the study relies on helical bending for

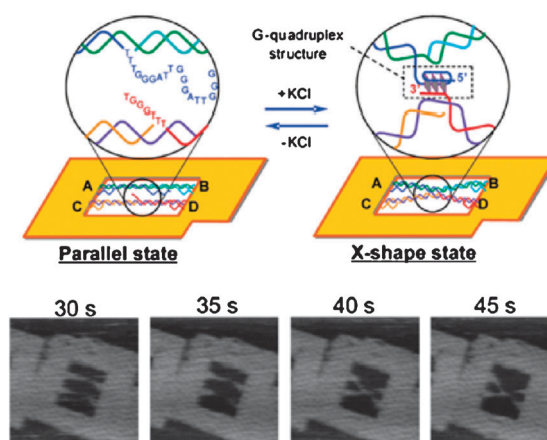


**Fig. 17** High-speed AFM enables the study of dynamic biomolecular events. Top: the addition of potassium ions facilitates the formation of a G-quadruplex. Bottom: G-quadruplex formation results in a connection between the two helices. This binding is observed in real time via high-speed AFM. Adapted with permission from ref. 70. Copyright 2010 American Chemical Society.

the catalytic reaction and the more relaxed double helix was shown to be more readily accessible to the enzymes.

Several exciting developments in molecular robotics have involved DNA origami platforms. Two reports of DNA walkers<sup>71</sup> following programmed paths on DNA origami<sup>72,73</sup> were published in the same issue of *Nature*. Seeman and co-workers described a system consisting of a triangular DNA-walker that walked between programmed stations upon the addition of specific oligonucleotides. Cargo (gold nanoparticles) could be picked up by the walker at the stations. Whether the cargo was transferred from the track to the walker was dependent on another set of oligonucleotides that controlled the conformation of each station. This complex system exhibited a previously unseen degree of functional control at the nanoscale. A schematic representation of the system is shown in Fig. 18a.

Stojanovic, Yan, Walter, Winfree and colleagues employed a so-called molecular spider consisting of a streptavidin body with three DNAzyme legs. The fourth streptavidin binding site contained a capture probe that was complementary to a docking station on the origami. A track for the molecular spiders was assembled on the surface of the origami by extending the staple strands with a specific sequence that is recognised and cleaved by the DNAzyme legs. A schematic representation is shown in Fig. 18b. As the spider moved forward the trailing track was degraded, resulting in unidirectional and completely autonomous movement. This movement was monitored by AFM and super resolution fluorescence microscopy.

More recently, a collaboration between the groups of Sugiyama and Turberfield investigated the movement of a restriction enzyme-driven walker by high-speed AFM.<sup>74</sup>

## Conclusion and perspective

Since the conceptual vision of structural DNA nanotechnology was laid out early in 1980s, followed by numerous fundamental steps in programming and engineering DNA nanostructures, and later the invention of the DNA origami

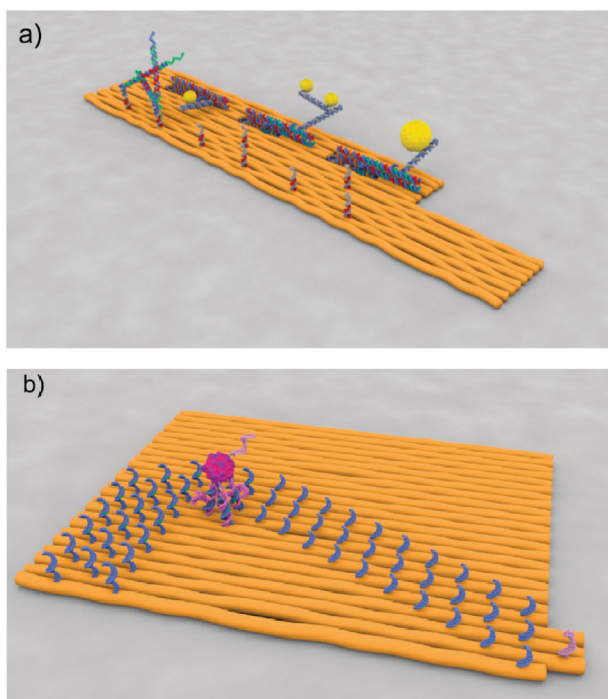


**Fig. 18** DNA walkers on origami tracks. (a) The Seeman walker picking up a gold nanoparticle. The triangular walker has three legs that will bind to different positions on the origami substrate depending on the addition of selected oligos. The walker arms can pick up gold nanoparticles if the stations are aligned correctly, this is also controlled by the addition of specific oligos. Inspiration by permission from MacMillan Publishers Ltd: ref. 72, copyright 2010. (b) The streptavidin spider from Yan and co-workers walking along a nucleic acid track. In this illustration the spider started in the lower right corner and has been walking along the track. The spider hydrolyses the track making its movement unidirectional and autonomous. Inspiration by permission from MacMillan Publishers Ltd: ref. 73, copyright 2010.<sup>73</sup>

technique, the field of structural DNA nanotechnology has undergone tremendous development. Today nanoscientists can create complex structures with almost any arbitrary shape and with precise addressability. The creation of higher order structures have been realised with polymerisation of origami monomers into two-dimensional arrays and a variety of functional components have been integrated to achieve even more complex constructions. The gap between top-down and bottom-up approaches has been significantly narrowed through precise deposition on patterned surfaces. Advanced real-time characterisations such as super resolution microscopy and high-speed AFM are widening the scope of potential applications even further.

The field still faces many challenges in the future. While various design methods allow the construction of complex 3D structures, the yields tend to fall as the complexity and density increases. While researchers are confronting this challenge, the lack of detailed information about the folding process is a key obstacle. Thorough investigations of the thermodynamics and kinetics of the DNA origami folding process are thus needed to provide valuable input for future designs of more complex structures and their hierarchical assemblies. Scaling up the origami assembly and thereby increasing the complexity has

been investigated by several research groups but much more work is still needed. To further explore the use of DNA origami as molecular chips for biological applications, stability and compatibility of these structures with biological samples need to be tested. Recently the labs of Yan *et al.*<sup>75</sup> and Dietz *et al.*<sup>76</sup> have reported stability investigations of DNA origami structures in biologically relevant environments, but *in vivo* experiments are still to be performed. The use of DNA origami as molecular rulers has opened up great opportunities for applications in biophysics and for real time studies of biomolecular processes. More work in this direction is much anticipated. In the past few years great improvements to achieve more robust conjugation between DNA nanostructures with inorganic nanomaterials and protein molecules have been obtained. Further progress is anticipated in making functional nanophotonic/nanoelectronic devices and spatially interacting protein networks in the coming years. Certainly, future progress in the field will entail interdisciplinary efforts from chemistry, biology, physics, material sciences, computer science and various engineering disciplines.

The invention of the DNA origami methodology has largely increased our ability to control self-assembly of complex structures. In this review we have described the remarkable development of the area in the first five years since the invention of DNA origami. Through several impressive contributions the power of this new technology to control matter at the nanoscale has been demonstrated and we believe that DNA origami holds great potential for future scientific and technological applications.

## Acknowledgements

Financial support for this work by the Danish National Research Foundation is gratefully acknowledged. Hao Yan was supported by grants from the Office of Naval Research, the Army Research Office, the National Science Foundation, Department of Energy, and National Institutes of Health. Hao Yan is part of the Center for Bio-Inspired Solar Fuel Production, an Energy Frontier Research Center funded by the US Department of Energy, Office of Science, Office of Basic Energy Sciences under Award Number DE-SC0001016.

## Notes and references

- 1 N. R. Kallenbach, R. I. Ma and N. C. Seeman, *Nature*, 1983, **305**, 829–831.
- 2 J. H. Chen and N. C. Seeman, *Nature*, 1991, **350**, 631–633.
- 3 E. Winfree, F. Liu, L. A. Wenzler and N. C. Seeman, *Nature*, 1998, **394**, 539–544.
- 4 J. Zheng, J. J. Birktoft, Y. Chen, T. Wang, R. Sha, P. E. Constantinou, S. L. Ginell, C. Mao and N. C. Seeman, *Nature*, 2009, **461**, 74–77.
- 5 P. W. K. Rothemund, *Nature*, 2006, **440**, 297–302.
- 6 W. M. Shih, J. D. Quispe and G. F. Joyce, *Nature*, 2004, **427**, 618–621.
- 7 T. J. Fu and N. C. Seeman, *Biochemistry*, 1993, **32**, 3211–3220.
- 8 S. M. Douglas, J. J. Chou and W. M. Shih, *Proc. Natl. Acad. Sci. U. S. A.*, 2007, **104**, 6644–6648.
- 9 S. M. Douglas, H. Dietz, T. Liedl, B. Hogberg, F. Graf and W. M. Shih, *Nature*, 2009, **459**, 414–418.
- 10 E. S. Andersen, M. D. Dong, M. M. Nielsen, K. Jahn, A. Lind-Thomsen, W. Mamdough, K. V. Gothelf, F. Besenbacher and J. Kjems, *ACS Nano*, 2008, **2**, 1213–1218.



- 11 S. M. Douglas, A. H. Marblestone, S. Teerapittayanon, A. Vazquez, G. M. Church and W. M. Shih, *Nucleic Acids Res.*, 2009, **37**, 5001–5006.
- 12 Y. Ke, S. M. Douglas, M. Liu, J. Sharma, A. Cheng, A. Leung, Y. Liu, W. M. Shih and H. Yan, *J. Am. Chem. Soc.*, 2009, **131**, 15903–15908.
- 13 L. Qian, Y. Wang, Z. Zhang, J. Zhao, D. Pan, Y. Zhang, Q. Liu, C. Fan, J. Hu and L. He, *Chin. Sci. Bull.*, 2006, **51**, 2973–2976.
- 14 E. S. Andersen, M. Dong, M. M. Nielsen, K. Jahn, R. Subramani, W. Mamdouh, M. M. Golas, B. Sander, H. Stark, C. L. Oliveira, J. S. Pedersen, V. Birkedal, F. Besenbacher, K. V. Gothelf and J. Kjems, *Nature*, 2009, **459**, 73–76.
- 15 A. Kuzuya and M. Komiyama, *Chem. Commun.*, 2009, 4182–4184.
- 16 M. Endo, K. Hidaka, T. Kato, K. Namba and H. Sugiyama, *J. Am. Chem. Soc.*, 2009, **131**, 15570–15571.
- 17 Y. G. Ke, J. Sharma, M. H. Liu, K. Jahn, Y. Liu and H. Yan, *Nano Lett.*, 2009, **9**, 2445–2447.
- 18 G. Bellot, M. A. McClintock, C. Lin and W. M. Shih, *Nat. Methods*, 2011, **8**, 192–194.
- 19 H. Dietz, S. M. Douglas and W. M. Shih, *Science*, 2009, **325**, 725–730.
- 20 D. Han, S. Pal, J. Nangreave, Z. Deng, Y. Liu and H. Yan, *Science*, 2011, **332**, 342–346.
- 21 T. Liedl, B. Hogberg, J. Tytell, D. E. Ingber and W. M. Shih, *Nat. Nanotechnol.*, 2010, **5**, 520–524.
- 22 D. R. Han, S. Pal, Y. Liu and H. Yan, *Nat. Nanotechnol.*, 2010, **5**, 712–717.
- 23 E. Pound, J. R. Ashton, H. A. Becerril and A. T. Woolley, *Nano Lett.*, 2009, **9**, 4302–4305.
- 24 I. Saaem, K. S. Ma, A. N. Marchi, T. H. LaBean and J. Tian, *ACS Appl. Mater. Interfaces*, 2010, **2**, 491–497.
- 25 R. D. Barish, R. Schulman, P. W. Rothmund and E. Winfree, *Proc. Natl. Acad. Sci. U. S. A.*, 2009, **106**, 6054–6059.
- 26 K. Fujibayashi, R. Hariadi, S. H. Park, E. Winfree and S. Murata, *Nano Lett.*, 2008, **8**, 1791–1797.
- 27 A. Rajendran, M. Endo, Y. Katsuda, K. Hidaka and H. Sugiyama, *ACS Nano*, 2011, **5**, 665–671.
- 28 W. Liu, H. Zhong, R. Wang and N. C. Seeman, *Angew. Chem., Int. Ed.*, 2011, **50**, 264–267.
- 29 Z. Zhao, H. Yan and Y. Liu, *Angew. Chem., Int. Ed.*, 2010, **49**, 1414–1417.
- 30 B. Hogberg, T. Liedl and W. M. Shih, *J. Am. Chem. Soc.*, 2009, **131**, 9154–9155.
- 31 R. Jungmann, T. Liedl, T. L. Sobey, W. Shih and F. C. Simmel, *J. Am. Chem. Soc.*, 2008, **130**, 10062–10063.
- 32 Z. Li, M. Liu, L. Wang, J. Nangreave, H. Yan and Y. Liu, *J. Am. Chem. Soc.*, 2010, **132**, 13545–13552.
- 33 Y. G. Ke, S. Lindsay, Y. Chang, Y. Liu and H. Yan, *Science*, 2008, **319**, 180–183.
- 34 Z. Zhang, D. Zeng, H. Ma, G. Feng, J. Hu, L. He, C. Li and C. Fan, *Small*, 2010, **6**, 1854–1858.
- 35 H. K. Subramanian, B. Chakraborty, R. Sha and N. C. Seeman, *Nano Lett.*, 2011, **11**, 910–913.
- 36 R. Chhabra, J. Sharma, Y. G. Ke, Y. Liu, S. Rinker, S. Lindsay and H. Yan, *J. Am. Chem. Soc.*, 2007, **129**, 10304–10305.
- 37 S. Rinker, Y. Ke, Y. Liu, R. Chhabra and H. Yan, *Nat. Nanotechnol.*, 2008, **3**, 418–422.
- 38 S. Pal, Z. Deng, B. Ding, H. Yan and Y. Liu, *Angew. Chem., Int. Ed.*, 2010, **49**, 2700–2704.
- 39 J. Sharma, R. Chhabra, C. S. Andersen, K. V. Gothelf, H. Yan and Y. Liu, *J. Am. Chem. Soc.*, 2008, **130**, 7820–7821.
- 40 B. Q. Ding, Z. T. Deng, H. Yan, S. Cabrini, R. N. Zuckermann and J. Bokor, *J. Am. Chem. Soc.*, 2010, **132**, 3248–3249.
- 41 L. A. Stearns, R. Chhabra, J. Sharma, Y. Liu, W. T. Petuskey, H. Yan and J. C. Chaput, *Angew. Chem., Int. Ed.*, 2009, **48**, 8494–8496.
- 42 Z. Zhao, E. L. Jacovetty, Y. Liu and H. Yan, *Angew. Chem., Int. Ed.*, 2011, **50**, 2041–2044.
- 43 H. T. Maune, S. P. Han, R. D. Barish, M. Bockrath, W. A. Goddard, P. W. K. Rothmund and E. Winfree, *Nat. Nanotechnol.*, 2010, **5**, 61–66.
- 44 H. Liu, T. Tørring, M. Dong, C. B. Rosen, F. Besenbacher and K. V. Gothelf, *J. Am. Chem. Soc.*, 2010, **132**, 18054–18056.
- 45 N. Stephanopoulos, M. H. Liu, G. J. Tong, Z. Li, Y. Liu, H. Yan and M. B. Francis, *Nano Lett.*, 2010, **10**, 2714–2720.
- 46 A. Kuzyk, K. T. Laitinen and P. Torma, *Nanotechnology*, 2009, **20**, 235305.
- 47 A. Kuzuya, M. Kimura, K. Numajiri, N. Koshi, T. Ohnishi, F. Okada and M. Komiyama, *ChemBioChem*, 2009, **10**, 1811–1815.
- 48 K. Numajiri, M. Kimura, A. Kuzuya and M. Komiyama, *Chem. Commun.*, 2010, **46**, 5127–5129.
- 49 W. Q. Shen, H. Zhong, D. Neff and M. L. Norton, *J. Am. Chem. Soc.*, 2009, **131**, 6660–6661.
- 50 K. Jahn, T. Tørring, N. V. Voigt, R. S. Sorensen, A. L. Bank Kodal, E. S. Andersen, K. V. Gothelf and J. Kjems, *Bioconjugate Chem.*, 2011, **22**, 819–823.
- 51 A. Kuzyk, B. Yurke, J. J. Toppari, V. Linko and P. Torma, *Small*, 2008, **4**, 447–450.
- 52 A. M. Hung, C. M. Micheel, L. D. Bozano, L. W. Osterbur, G. M. Wallraff and J. N. Cha, *Nat. Nanotechnol.*, 2010, **5**, 121–126.
- 53 B. Q. Ding, H. Wu, W. Xu, Z. A. Zhao, Y. Liu, H. B. Yu and H. Yan, *Nano Lett.*, 2010, **10**, 5065–5069.
- 54 R. J. Kershner, L. D. Bozano, C. M. Micheel, A. M. Hung, A. R. Fornof, J. N. Cha, C. T. Rettner, M. Bersani, J. Frommer, P. W. K. Rothmund and G. M. Wallraff, *Nat. Nanotechnol.*, 2009, **4**, 557–561.
- 55 A. E. Gordon, S. S. Oh, K. Hsieh, Y. Ke, H. Yan and H. T. Soh, *Small*, 2009, **5**, 1942–1946.
- 56 S. Pal, R. Varghese, Z. Deng, Z. Zhao, A. Kumar, H. Yan and Y. Liu, *Angew. Chem., Int. Ed.*, 2011, **50**, 4176–4179.
- 57 J. F. Liu, Y. L. Geng, E. Pound, S. Gyawali, J. R. Ashton, J. Hickey, A. T. Woolley and J. N. Harb, *ACS Nano*, 2011, **5**, 2240–2247.
- 58 R. Schreiber, S. Kempter, S. Holler, V. Schüller, D. Schiffels, S. S. Simmel, P. S. Nickels and T. Liedl, *Small*, 2011, DOI: 10.1002/smll.201100465.
- 59 N. V. Voigt, T. Tørring, A. Rotaru, M. F. Jacobsen, J. B. Ravnsbaek, R. Subramani, W. Mamdouh, J. Kjems, A. Mokhir, F. Besenbacher and K. V. Gothelf, *Nat. Nanotechnol.*, 2010, **5**, 200–203.
- 60 S. Helmig, A. Rotaru, D. Arian, L. Kovbasyuk, J. Arnbjerg, P. R. Ogilby, J. Kjems, A. Mokhir, F. Besenbacher and K. V. Gothelf, *ACS Nano*, 2010, **4**, 7475–7480.
- 61 B. Sacca, R. Meyer, M. Erkelenz, K. Kiko, A. Arndt, H. Schroeder, K. S. Rabe and C. M. Niemeyer, *Angew. Chem., Int. Ed.*, 2010, **49**, 9378–9383.
- 62 K. Numajiri, T. Yamazaki, M. Kimura, A. Kuzuya and M. Komiyama, *J. Am. Chem. Soc.*, 2010, **132**, 9937–9939.
- 63 R. Subramani, S. Juul, A. Rotaru, F. F. Andersen, K. V. Gothelf, W. Mamdouh, F. Besenbacher, M. Dong and B. R. Knudsen, *ACS Nano*, 2010, **4**, 5969–5977.
- 64 C. Steinhauer, R. Jungmann, T. L. Sobey, F. C. Simmel and P. Tinnefeld, *Angew. Chem., Int. Ed.*, 2009, **48**, 8870–8873.
- 65 R. Jungmann, C. Steinhauer, M. Scheible, A. Kuzyk, P. Tinnefeld and F. C. Simmel, *Nano Lett.*, 2010, **10**, 4756–4761.
- 66 I. H. Stein, C. Steinhauer and P. Tinnefeld, *J. Am. Chem. Soc.*, 2011, **133**, 4193–4195.
- 67 I. H. Stein, V. Schuller, P. Bohm, P. Tinnefeld and T. Liedl, *ChemPhysChem*, 2011, **12**, 689–695.
- 68 M. Endo, Y. Katsuda, K. Hidaka and H. Sugiyama, *J. Am. Chem. Soc.*, 2010, **132**, 1592–1597.
- 69 M. Endo, Y. Katsuda, K. Hidaka and H. Sugiyama, *Angew. Chem., Int. Ed.*, 2010, **49**, 9412–9416.
- 70 Y. Sannohe, M. Endo, Y. Katsuda, K. Hidaka and H. Sugiyama, *J. Am. Chem. Soc.*, 2010, **132**, 16311–16313.
- 71 H. Liu and D. Liu, *Chem. Commun.*, 2009, 2625–2636.
- 72 H. Gu, J. Chao, S. J. Xiao and N. C. Seeman, *Nature*, 2010, **465**, 202–205.
- 73 K. Lund, A. J. Manzo, N. Dabby, N. Michelotti, A. Johnson-Buck, J. Nangreave, S. Taylor, R. Pei, M. N. Stojanovic, N. G. Walter, E. Winfree and H. Yan, *Nature*, 2010, **465**, 206–210.
- 74 S. F. Wickham, M. Endo, Y. Katsuda, K. Hidaka, J. Bath, H. Sugiyama and A. J. Turberfield, *Nat. Nanotechnol.*, 2011, **6**, 166–169.
- 75 Q. Mei, X. Wei, F. Su, Y. Liu, C. Youngbull, R. Johnson, S. Lindsay, H. Yan and D. Meldrum, *Nano Lett.*, 2011, **11**, 1477–1482.
- 76 C. E. Castro, F. Kilchherr, D. N. Kim, E. L. Shiao, T. Wauer, P. Wortmann, M. Bathe and H. Dietz, *Nat. Methods*, 2011, **8**, 221–229.